The Advanced Virgo detector

2015 J. Phys.: Conf. Ser. 610 012014

(http://iopscience.iop.org/1742-6596/610/1/012014)

The Advanced Virgo detector

F. Acernese[35,11], T. Adams[19], M. Agathos[23], K. Agatsuma[23], A. Allocca[36,14], P. Astone[15], G. Ballardin[5], F. Barone[35,11], M. Barsuglia[1], A. Basti[31,14], Th. S. Bauer[23], V. Bavigadda[5], M. Bejger[4], C. Belczynski[3], D. Bersanetti[28,9], A. Bertolini[23], M. Bitossi[5,14], M. A. Bizouard[18], S. Bloemen[23,24], M. Boer[2], G. Bogaert[2], F. Bondu[32], L. Bonelli[31,14], R. Bonnand[19], V. Boschi[14], L. Bosi[13], C. Bradaschia[14], M. Branchesi[38,8], T. Briant[20], A. Brillet[2], V. Brisson[18], T. Bulik[3], H. J. Bulten[26,23], D. Buskulic[19], C. Buy[1], G. Cagnoli[21], E. Calloni[29,11], F. Carbognani[5], F. Cavalier[18], R. Cavalieri[5], G. Cella[14], E. Cesarini[16], E. Chassande-Mottin[1], A. Chincarini[9], A. Chiummo[5], S. Chua[20], F. Cleva[2], E. Coccia[34,10], P.-F. Cohadon[20], A. Colla[33,15], M. Colombini[13], A. Conte[33,15], J.-P. Coulon[2], E. Cuoco[5], S. D'Antonio[16], V. Dattilo[5], M. Davier[18], R. Day[5], G. Debreczeni[25], J. Degallaix[21], M. De Laurentis[29,11], S. Deléglise[20], W. Del Pozzo[23], H. Dereli[2], R. De Rosa[29,11], L. Di Fiore[11], A. Di Lieto[31,14], A. Di Virgilio[14], V. Dolique[21], M. Drago[37,17], M. Ducrot[19], G. Endrőczi[25], V. Fafone[34,16], S. Farinon[9], I. Ferrante[31,14], F. Ferrini[5], F. Fidecaro[31,14], I. Fiori[5], R. Flaminio[21], J.-D. Fournier[2], S. Franco[18], S. Frasca[33,15], F. Frasconi[14], L. Gammaitoni[30,13], F. Garufi[29,11], A. Gatto[1], G. Gemme[9], B. Gendre[2], E. Genin[5], A. Gennai[14], S. Ghosh[23,24], A. Giazotto[14], R. Gouaty[19], M. Granata[21], G. Greco[8,38], P. Groot[24], G. M. Guidi[38,8], J. Harms[8], A. Heidmann[20], H. Heitmann[2], P. Hello[18], G. Hemming[5], D. Hofman[21], R.J.G. Jonker[23], M. Kasprzack[18,5], F. Kéfélian[2], A. Królak[22,7], A. Kutynia[22], C. Lazzaro[12], E. Lebigot[1], M. Leonardi[37,17], N. Leroy[18], N. Letendre[19], M. Lorenzini[34,16], V. Loriette[6], G. Losurdo[8], E. Majorana[15], I. Maksimovic[6], V. Malvezzi[34,16], N. Man[2], V. Mangano[33,15], M. Mantovani[5,14], F. Marchesoni[27,13], F. Marion[19], J. Marque[5], F. Martelli[38,8], L. Martinelli[2], A. Masserot[19], D. Meacher[2], J. Meidam[23], F. Mezzani[15,33], C. Michel[21], L. Milano[29,11], Y. Minenkov[16], A. Moggi[14], M. Mohan[5], B. Mours[19], M. F. Nagy[25], I. Nardecchia[34,16], L. Naticchioni[33,15], G. Nelemans[23,24], I. Neri[30,13], M. Neri[28,9], F. Nocera[5], C. Palomba[15], F. Paoletti[5,14], A. Pasqualetti[5], R. Passaquieti[31,14], D. Passuello[14], M. Pichot[2], F. Piergiovanni[38,8], G. Pillant[5], L. Pinard[21], R. Poggiani[31,14], M. Prijatelj[5], G. A. Prodi[37,17],

M. Punturo[13], P. Puppo[15], D. S. Rabeling[26,23], I. Rácz[25], P. Rapagnani[33,15], M. Razzano[31,14], V. Re[34,16], T. Regimbau[2], F. Ricci[33,15], F. Robinet[18], A. Rocchi[16], L. Rolland[19], R. Romano[35,11], P. Ruggi[5], B. Sassolas[21], D. Sentenac[5], V. Sequino[34,16], S. Shah[23,24], K. Siellez[2], N. Straniero[21], B. Swinkels[5], M. Tacca[1], M. Tonelli[31,14], F. Travasso[30,13], G. Vajente[31,14], N. van Bakel[23], M. van Beuzekom[23], J. F. J. van den Brand[26,23], C. Van Den Broeck[23], M. V. van der Sluys[23,24], J. van Heijningen[23], M. Vasúth[25], G. Vedovato[12], J. Veitch[23], D. Verkindt[19], F. Vetrano[38,8], A. Viceré[38,8], J.-Y. Vinet[2], H. Vocca[30,13], L.-W. Wei[2], M. Yvert[19], A. Zadrożny[22], J.-P. Zendri[12]

[1]APC, AstroParticule et Cosmologie, Université Paris Diderot, CNRS/IN2P3, CEA/Irfu, Observatoire de Paris, Sorbonne Paris Cité, 10, rue Alice Domon et Léonie Duquet, F-75205 Paris Cedex 13, France
[2]ARTEMIS, Université Nice-Sophia-Antipolis, CNRS and Observatoire de la Côte d'Azur, F-06304 Nice, France
[3]Astronomical Observatory Warsaw University, 00-478 Warsaw, Poland
[4]CAMK-PAN, 00-716 Warsaw, Poland
[5]European Gravitational Observatory (EGO), I-56021 Cascina, Pisa, Italy
[6]ESPCI, CNRS, F-75005 Paris, France
[7]IM-PAN, 00-956 Warsaw, Poland
[8]INFN, Sezione di Firenze, I-50019 Sesto Fiorentino, Firenze, Italy
[9]INFN, Sezione di Genova, I-16146 Genova, Italy
[10]INFN, Gran Sasso Science Institute, I-67100 L'Aquila, Italy
[11]INFN, Sezione di Napoli, Complesso Universitario di Monte S.Angelo, I-80126 Napoli, Italy
[12]INFN, Sezione di Padova, I-35131 Padova, Italy
[13]INFN, Sezione di Perugia, I-06123 Perugia, Italy
[14]INFN, Sezione di Pisa, I-56127 Pisa, Italy
[15]INFN, Sezione di Roma, I-00185 Roma, Italy
[16]INFN, Sezione di Roma Tor Vergata, I-00133 Roma, Italy
[17]INFN, Trento Institute for Fundamental Physics and Applications, I-38123 Povo, Trento, Italy
[18]LAL, Université Paris-Sud, IN2P3/CNRS, F-91898 Orsay, France
[19]Laboratoire d'Annecy-le-Vieux de Physique des Particules (LAPP), Université de Savoie, CNRS/IN2P3, F-74941 Annecy-le-Vieux, France
[20]Laboratoire Kastler Brossel, ENS, CNRS, UPMC, Université Pierre et Marie Curie, F-75005 Paris, France
[21]Laboratoire des Matériaux Avancés (LMA), IN2P3/CNRS, Université de Lyon, F-69622 Villeurbanne, Lyon, France
[22]NCBJ, 05-400 Świerk-Otwock, Poland
[23]Nikhef, Science Park, 1098 XG Amsterdam, The Netherlands
[24]Department of Astrophysics/IMAPP, Radboud University Nijmegen, P.O. Box 9010, 6500 GL Nijmegen, The Netherlands
[25]Wigner RCP, RMKI, H-1121 Budapest, Konkoly Thege Miklós út 29-33, Hungary
[26]VU University Amsterdam, 1081 HV Amsterdam, The Netherlands
[27]Università di Camerino, Dipartimento di Fisica, I-62032 Camerino, Italy
[28]Università degli Studi di Genova, I-16146 Genova, Italy
[29]Università di Napoli 'Federico II', Complesso Universitario di Monte S.Angelo, I-80126 Napoli, Italy
[30]Università di Perugia, I-06123 Perugia, Italy
[31]Università di Pisa, I-56127 Pisa, Italy
[32]Institut de Physique de Rennes, CNRS, Université de Rennes 1, F-35042 Rennes, France
[33]Università di Roma 'La Sapienza', I-00185 Roma, Italy

[34]Università di Roma Tor Vergata, I-00133 Roma, Italy
[35]Università di Salerno, Fisciano, I-84084 Salerno, Italy
[36]Università di Siena, I-53100 Siena, Italy
[37]Università di Trento, I-38123 Povo, Trento, Italy
[38]Università degli Studi di Urbino 'Carlo Bo', I-61029 Urbino, Italy

E-mail: paola.puppo@roma1.infn.it

Abstract. The Advanced Virgo interferometer is the upgraded version of the Virgo detector having the goal to extend by a factor 10 the observation horizon in the universe and consequently increase the detection rate by three orders of magnitude. Its installation is in progress and is expected to be completed in late 2015. In this proceeding we will present the scheme and the main challenging technical features of the detector and we will give an outline of the installation status and the foreseen time schedule which will bring Advanced Virgo to its full operation.

PACS numbers: 04.80.Nn, 95.55.Ym, 95.75.Kk

1. Introduction

Advanced Virgo (AdV) is the largest European gravitational-wave detector located at the European Gravitational Observatory (EGO) site in the Pisa countryside (Italy). In the last 10 years, the Virgo collaboration has been extended from Italy and France to three other european countries: Holland, Poland and Hungary, and it now includes up to 19 laboratories in Europe.

In March 2014 a Memorandum of Understanding for full data exchange, joint data analysis and publication policy was signed with the LIGO Scientific Collaboration, thus continuing a world wide network of second generation detectors (including Advanced Virgo, the two Advanced LIGO [1], GEO HF [2]).

2. Advanced Virgo main upgrades

Advanced Virgo (AdV) is the project to upgrade the Virgo detector [3] to a second generation instrument. It is designed with the aim to increase the sensitivity of about one order of magnitude and consequently extend the amount of probed Universe of a factor thousand. The Virgo detector upgrade passed through an intermediate step, named as Virgo+, in which some technical improvements were applied. They include the increase of the laser power up to 25 Watts and the introduction of the thermal compensation system to correct the thermal lensing effects. A second action was the use of silica fibres to suspend the mirrors for the reduction of the suspensions thermal noise. Finally, increasing the Finesse of the cavities from 50 to 150 completed this step. The Virgo+ detector has been run from 2010 up to the end of 2012 in coincidence with the Enhanced LIGO detectors[1].

The upgrade to AdV has been funded and started in 2009, and it is planned to finish in fall 2015 when the commissioning of the interferometer will start. This planning should allow a first science run data taking to be started in mid-2016.

2.1. Interferometer optical configuration and features

Advanced Virgo is a dual recycled interferometer as shown in fig. 2 of the introductory overview of this issue [6]. The detector will be illuminated by a 200 W laser beam delivering 125 W at the entrance of the interferometer. The optical power inside the power recycling cavity, at the beamsplitter will be 5 kW and up to 700 kW of light will be stored in the arms. Compared to Virgo, the light circulating in the arm cavities will be increased by a factor 350.

The choice of the arm cavities features deals with the aimed reduction of the mirror coating thermal noise which dominates in the mid-frequency range, of the thermal gradients on the mirror surface and of the alignment instabilities induced by the radiation pressure effect. To reduce the coating thermal noise the beam waist has been increased with respect to Virgo from 2 cm to 5 cm. With the 350 mm mirror diameters, such a value ensures negligible beam clipping losses (below 1 ppm). Moreover the beam waist will be placed in the center of the Fabry-Perot cavities nearer the input masses resulting in a larger beam size on the End Mirror (5.8 cm) than on the Input Mirror (4.87 cm) allowing the coating thermal noise of all the test masses to give an optimized contribution to the sensitivity curve.

Advanced Virgo will use marginally stable recycling cavities. The choice is driven by the construction schedule, the budget and the increased suspension complexity that would have to be required by a non degenerate-cavity solution like that one adopted in Advanced LIGO [1]. This configuration combined with the enlarged beam size is more sensitive to thermal effects on the mirror surfaces and to the aberrations due to their fabrication defects. However, a new mirror technology has been developed so that high performance optics are employed and a very sophisticated correction system of the thermal aberrations was set up to on purpose.

A new kind of substrate (Suprasil 3001/3002) is employed to make the cavity mirrors, so that the optical absorption is 3 times lower than in Virgo. Thanks to a new coating system, both the ITM and ETM mirrors are produced in pairs, as a consequence the asymmetry between the interferometer cavities is made nearly negligible. Moreover the use of Ti doped Ta_2O_5 as higher optical index material and the optimized layers thicknesses for the coating gives good results for the reduction of the mechanical and optical loss factors [4, 5].

With the signal recycling technique the detector response depends mainly on the properties of the signal recycling cavity and on the circulating power. The arm cavity finesse of about 450, the power recycling and signal recycling mirror transmissions respectively of 5% and 20% are chosen as a trade off between maximizing the circulating power and reducing the aberration effects, thus allowing the sensitivity to be optimized in a chosen sensitivity bandwidth.

To make a initial locking of the full interferometer an auxiliary green laser will be used, which will see lower cavity finesses easing the locking procedure. The mirror coatings are designed to have the optical properties suitable for this purpose.

2.2. Dealing with the high power stored in the cavities

Although the quantity of power absorbed by the highly improved quality mirror substrates and coatings is very small (0.3-0.4 ppm), the big amount of power in the cavity is sufficient to produce a non negligible thermal lensing effect which can spoil the laser beam matching in the cavities and degrade the interferometer performance

[7]. This effect is mainly due to the heat absorption in the mirror bulk and coatings and to reduce it a thermal compensation system (TCS), successfully used in Virgo+, has been designed and improved to deal with the new higher power [8].

In Advanced Virgo the TCS will need to correct the optical aberrations in the power recycling cavity and to correct the radius of curvature of all the test masses [9, 10]. Indeed, the inhomogeneous heating of the mirror surfaces will produce a change of their curvature radius and produce a distortion in the light beam wavefront via the thermo-elastic effect on the mirror coatings. A useful way to picture the optical distortion effect, is to use the fractional power scattered out from the TEM_{00} mode [11, 12], termed coupling losses, and the Gaussian-weighted RMS of the optical path length increase. To allow a correct operation of the detector, the coupling losses due to the thermal lensing must be reduced at least of a factor 10^3, this value should result in a reduction of the RMS fluctuations of the optical paths of 2 nm . The adjustment of the mirrors radius of curvature is provided with the use of heating rings surrounding the test masses on their back side. Moreover an appropriate heating pattern generated by a CO_2 laser which is completely absorbed by the fused silica substrates will be used. This last solution was tested during the Virgo+ operation by projecting a CO_2 laser beam in annulus shape on the mirror. However, in AdV the use of a higher power correcting CO_2 beam on the mirrors could introduce a displacement noise due to its intensity fluctuation, for this reason an additional transmissive optic (named Compensation Plates) is employed and placed on the mirrors back side, in the recycling cavities, avoiding any direct coupling effect of its motion to the dark fringe. The studies of the corrective patterns have been carried out with Finite Element Models so that it was possible to define an optimal corrective procedure that would allow the optical path RMS to be reduced by a factor 20 down to 0.35 nm, well within the requirements. The sensing system used in the TCS have been set up employing Hartmann wavefront sensors and phase cameras to detect the production of spurious light modes [**?**, 14].

2.3. Dealing with the stray light

A small amount of the power circulating in the interferometer is backscattered by all the illuminated surfaces. This effect becomes very important in the second generation interferometer with a bigger circulating power [15]. The stray light can increase the phase noise and spoil the sensitivity. To deal with such a problem diaphragm baffles are mounted around the suspended mirrors and placed at the vacuum tubes entrances and inside the links where the stray beams can be more noisy. They are designed to intercept and absorb as much as possible the stray light. For this reason they must have low scattering and low reflectivity features, and where required they must be suspended so that the residual injected strain noise is kept negligible. In AdV the baffles are stainless steel plates coated with Diamond-like Carbon, ensuring an acceptable damage threshold of 0.5 kW/cm^2, the choice was driven by a compromise between the requirements and the costs.

The scattered light that could arise from all the photodiodes used for the interferometer diagnostics and locking and for the signal detection and injection during the scientific runs will be reduced by suspending all the optical benches in vacuum. The five optical benches placed at the two cavity ends, at the power recycling pick off port and at the injection and detection systems are hung from five multistage vibration isolators (minitowers). This solution makes the interferometer less vulnerable to the

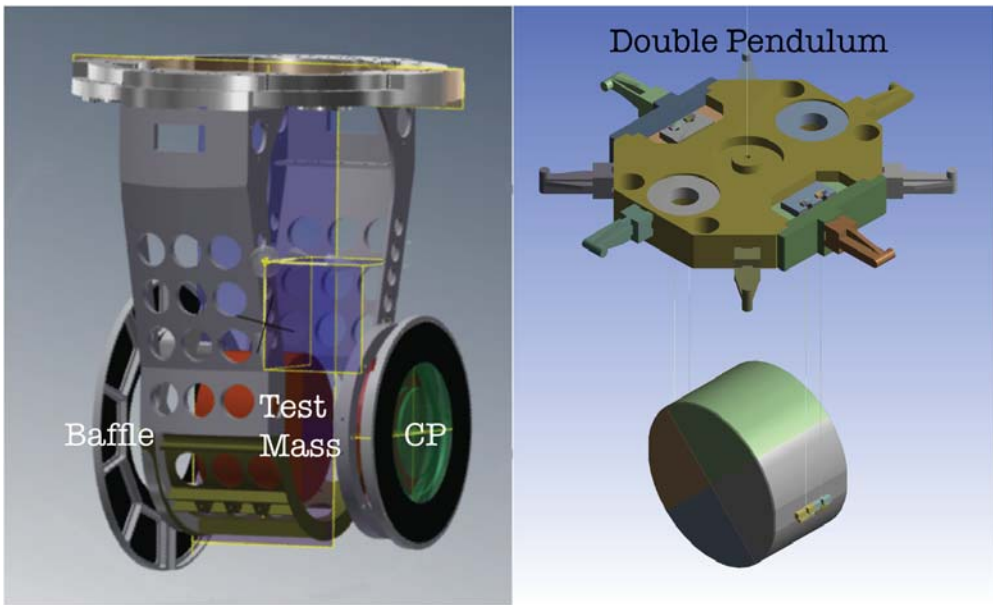

Figure 1. The new payloads in AdV must be compliant with the presence of the baffles and the TCS elements and with the double stage mirror monolithic suspension.

effect of the upconversion of the scattered light due to the seismic motion.

2.4. The mirror suspension system

In AdV heavier test masses of (42 kg) with the same diameter (350 mm) as in Virgo but a doubled thickness (20 cm) will be adopted. This solution is crucial to decrease the radiation pressure noise effect due to the high power circulating into the interferometer cavities. Moreover, the enlarged beam will require a larger beam splitter having a diameter of 550 mm with a total weigth of 34 kg.

All the test masses are suspended from a double pendulum stage (right picture in the figure 1) through the low loss silica fibers having a diameter of 400 μm whose profile has also been optimized to reduce the thermoelastic losses and consequently decrease the suspension thermal noise. Profiting from the experience gained in Virgo+[18, 19], the design of the fiber clamping systems both on the mirrors and on the intermediate suspension stages were improved to deal with the silica-steel interfaces, which can be a thermal noise source[16, 17]. All these clamping systems rely on the well known and tested silicate bonding technique which can reproduce the connection between materials at the molecular level and for this reason we talk of monolithic suspension system [20].

The mirror last stage suspension (payload), used to control the test masses and equipped with the sensors and actuators for the local and global control purposes, must be compliant with the monolithic suspension system, with the presence of the baffles and of the TCS elements. For this reason this part has been completely redesigned (left picture in the figure 1), and a big effort to improve the mechanical features has been made with help of the FEM. The study was crucial for defining the CP supporting

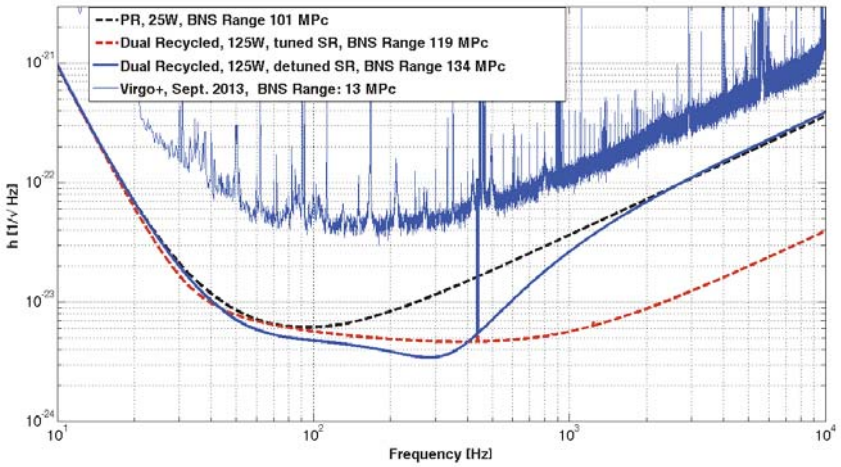

Figure 2. AdV sensitivity for the three configuration foreseen for the advanced detector step by step commissiong procedure in the Advanced Virgo technical design report (TDR) [23]. The early operation (black dashed line) with 25 W input power and without signal recycling, the mid-term operation with 125 W laser and tuned SRM (red dashed line), the early operation with 125 W laser and detuned SRM (solid blue line). For comparison the best noise sensitivity obtained in Virgo+ is shown.

system without adding extra displacement noise to the ITF output signal [21].

Moreover the superattenuators providing the seismic isolation whose performances have been widely demonstrated in Virgo [22], have been improved to be coupled with the new payloads. In particular new steering filters have been produced and the possibility to actively control the tilts induced by the seismic motion is being implemented.

2.5. Important infrastructure upgrades

The AdV infrastructure is essentially the same as for the Virgo detector. However some important improvements have been done in the central hall to host the minitowers, and to turn the laser and detection lab into acoustically isolated clean rooms. Large cryotraps are being installed at the end of the vacuum links to improve the residual pressure by a factor 100. Finally, several upgrades on the data acquisition and electronic systems will be done to handle the increased number of channels due to the new dual recycling control scheme.

3. The sensitivity of AdV

The peak sensitivity of Advanced Virgo is expected to be $3.4 \times 10^{-24}\ 1/\sqrt{\text{Hz}}$ around 300 Hz. This value refers to the target sensitivity presented in the Advanced Virgo Technical Design Report (TDR) [23] approved by the funding agencies in 2012 and shown in figure 2 (solid blue line) and compared also with the other second generation detector sensitivities in the figure 3 of the introductory overview in this issue. The expected inspiral range which can be derived from this sensitivity, is 140 Mpc for

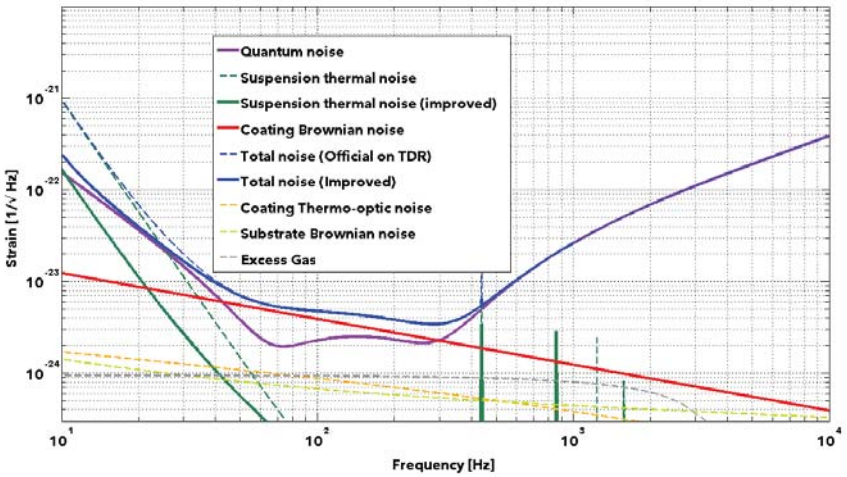

Figure 3. The official AdV sensitivity (blue dotted line) compared with the noise budget projection (blue solid line) based on the new improvements introduced in the detector design and modeling. With the new suspension design the thermal noise is improved by an order of magnitude in the low frequency range (green dotted line compared with the solid green line). In the mid-frequency range the noise is dominated by the coating thermal noise. Some other technical noise sources are sketched

binary neutron stars (BNS) of 1.5 $M_\odot$ and 1 Gpc for coalescing binaries black holes (BBH) of 30 $M_\odot$. In the figure 2 are also shown the two other sensitivity stages that Advanced Virgo pass through as mid-steps to reach its final operation. Indeed, AdV will not be operated in the final configuration at the beginning, and to face the problems arising from the new features, a step by step approach will be carried on. The planning is to have an early configuration with the power recycled detector using the initial Virgo+ 25 W laser, and no SR mirror (black dashed line) very similar to the former Virgo detector and easier to deal with. Then, after the installation of the new powerful laser, a mid-term dual-recycled configuration with a high power laser of 125 W and a tuned SR (red dashed line) will be followed by the configuration with a high power laser of 125 W and a detuned SR allowing the targeted sensitivity to be reached (solid blue line). The commissioning periods will be alternated with periods of data taking in coordination with Advanced LIGO in order to maximize the network capabilities.

3.1. Some improvement on the noise budget.

The main contributors to the sensitivity curve are the suspension thermal noise, the coating thermal noise up to 300 Hz, and then the quantum noise [23]. Since the TDR release some progress was made both in the design of the detector and in the modeling of the noise. The first tests of the new BS payloads, similar to the test mass payloads, showed a big improvement in the dissipation of the second stage suspension. Thanks to this result we are able to make a more optimistic projection of the AdV noise budget in this zone as it is sketched in the sensitivity curve shown in figure 3.

4. Status and Conclusions

At the time of writing, during the summer 2014, the installation of the interferometer optics has started. The injection bench and the mode cleaner far mirror were installed and their commissioning is started. Moreover the Beam Splitter payload assembly is succesfully finished and it is ready to be integrated in the tower by the end of September. The important infrastructure work was completed in October 2013 and the equipment installation is in progress.

The main mirrors of Advanced Virgo are being coated and characterized and the two input masses will be ready for their installation on site at the end of 2014. The commissioning of the new interferometer will start in mid-2015 and will last around 6 months with first a configuration similar to Virgo+ (25 W of input power and no signal recycling effect). The goal is to have an interferometer ready to participate in the first science run in coincidence with the Advanced LIGO interferometers in 2016. As a last step the input power will be raised gradually to 200 W and the signal recycling will be installed to allow the detector to reach its maximal sensitivity.

References

[1] S Dwyer and the LIGO Scientific Collaboration 2014 *Journal of Physics: Conference Series to be published in this issue.*
[2] K L Dooley and the LIGO Scientific Collaboration 2014 *Journal of Physics: Conference Series to be published in this issue.*
[3] The Virgo collaboration 2012 *JINST* **7** 3012
[4] C.Comtet et al., Proceedings of the 42th Rencontres de Moriond, 2007.
[5] Cimma, D. Forest, P. Ganau, B. Lagrange, J.M. Mackowski, C. Michel, J.L. Montorio, N. Morgado, R. Pignard, L. Pinard, A. Remillieux, Applied Optics, vol. 45 7 (2006) 1436-1439.
[6] K L Dooley, T Akutsu, S Dwyer, P Puppo 2014 *Journal of Physics: Conference Series to be published in this issue.*
[7] Hello P and Vinet J 1993 *Phys. Lett. A* **178** 351
[8] L. Pinard, R. Flaminio, D. Forest, *Bulk absorption measurement at 1064 nm of the new Heraeus ultra pure fused silica used for the Advanced Virgo Test Mass: effect of the annealing*, Virgo note VIR-0091A-10 (URL https://tds.ego-gw.it/ql/?c=7215) (2010).
[9] F. Acernese et al., J. Phys.: Conf. Ser. 120, 032007 (2008).
[10] T. Accadia et al., Proceedings of the 12th Marcell Grossmann Meeting ed T Damour, R T Jantzen and R Ruffini (Singapore: World Scientific) (2011).
[11] P. Hello, Eur. Phys. J. D 15, 373-383 (2001) .
[12] J.Y. Vinet, Living Rev. Relativity, 12, 5 (2009).
[13] A. Rocchi et al., J. P. Conf. Series 363, 012016 (2012).
[14] R. Day, Simulation of use of phase camera as sensor for correcting common high order aberrations in MSRC, VIR-0389A-11 (2011).
[15] A.Chiummo, R.Day, J.Marque, AdV - Stray Light Control: Requirements for wide-angle scattering in the arm cavity, VIR-0055A-13 URL https://tds.ego-gw.it/ql/?c=9398
[16] G. Cagnoli G. et al., Physical Letters A, vol. 255, p. 230, 1999
[17] Y. L. Huang, P. R. Saulson P. R., Review Scientific Instruments, vol. 69, p. 544, 1997
[18] T. Accadia et al., Class. Quantum Grav. 28 (2011) (doi:10.1088/0264-9381/28/11/114002)
[19] P. Puppo, M. Colombini, I. Nardecchia, E. Majorana, P. Rapagnani, F. Ricci: Virgo+ Thermal Noise Study, VIR-0074B-12, June 13 (2012), URL https://tds.ego-gw.it/ql/?c=8878
[20] G. Cagnoli et al., Physical Review Letters, vol. 85, p. 2442, 2000
[21] Conte, P. Puppo, P. Rapagnani: Thermal Noise evaluation of the Compensation Plate, Virgo internal note: VIR-0469A-13, October 24 (2013), URL https://tds.ego-gw.it/ql/?c=9851
[22] Braccini S *et al.* 2005 *Astroparticle Physics* **23** 557
[23] Collaboration T V 2012 Advanced Virgo technical design report, VIR-0128A-12 URL https://tds.ego-gw.it/ql/?c=8940